

# Long term stability and dynamical environment of the PSR 1257+12 planetary system

Krzysztof Goździewski<sup>1</sup>

*Toruń Centre for Astronomy, N. Copernicus University, Gagarina 11, 87-100 Toruń, Poland*

Maciej Konacki<sup>2</sup>

*Department of Geological and Planetary Sciences, California Institute of Technology, MS 150-21,  
Pasadena, CA 91125, USA*

*Nicolaus Copernicus Astronomical Center, Polish Academy of Sciences, Rabiańska 8, 87-100 Toruń,  
Poland*

Alex Wolszczan<sup>3</sup>

*Department of Astronomy and Astrophysics, Penn State University, University Park, PA 16802, USA  
Toruń Centre for Astronomy, Nicolaus Copernicus University ul. Gagarina 11, 87-100 Toruń, Poland*

## ABSTRACT

We study the long-term dynamics of the PSR 1257+12 planetary system. Using the recently determined accurate initial condition by Konacki & Wolszczan (2003) who derived the orbital inclinations and the absolute masses of the planets, we investigate the system stability by long-term, 1 Gyr direct integrations. No secular changes of the semi-major axes, eccentricities and inclinations appear during such an interval. This stable behavior is confirmed with the fast indicator MEGNO. The analysis of the orbital stability in the neighborhood of the nominal initial condition reveals that the PSR 1257+12 system is localized in a wide stable region of the phase space. Another feature confirming the long term stability is a negligible exchange of the Angular Momentum Deficit between the innermost planet A and the pair of the outer planets B and C. An important factor for maintaining the stability is also the presence of the secular apsidal resonance (SAR) between the planets B and C with the center of libration about 180°. SAR has been recently found in many extrasolar systems discovered by the radial velocity surveys (Ji et al. 2003). The fact that it is present both in planetary systems around main-sequence stars and around a neutron star may suggest that it is a common dynamical feature of exosystems. We also perform a preliminary study of the short-term dynamics of massless particles in the system. It uncovers a relatively extended stable zone between the planets A and B. Beyond the planet C, the stable zone starts already at distances 0.5 AU from the parent

---

<sup>1</sup>e-mail: k.gozdziewski@astri.uni.torun.pl

<sup>2</sup>e-mail: maciej@gps.caltech.edu

<sup>3</sup>e-mail: alex@astro.psu.edu

star. For moderately low eccentricities, beyond 1 AU, the motion of massless particles does not suffer from strong instabilities and this zone is basically stable, independent on the inclinations of the orbits of the test particles to the mean orbital plane of the system. It is a very encouraging result supporting the search for a putative dust disk or a Kuiper belt, especially with the SIRTF mission.

*Subject headings:* celestial mechanics, stellar dynamics—methods: numerical, N-body simulations—planetary systems—stars: individual (PSR 1257+12)

## 1. Introduction

Up to date, among about 110 extrasolar planetary systems, the one around PSR 1257+12 remains the only confirmed exosystem which contains Earth-sized planets (Wolszczan & Frail 1992; Wolszczan 1994; Konacki & Wolszczan 2003). It has been discovered with the pulsar timing technique that relies on extremely precise measurements of the times of arrival (TOA) of pulsar pulses. Such a technique in principle allows a detection of companions as small as asteroids. In the case of the PSR B1257+12 it enabled the detection of three planets A, B and C with the orbital periods of 25, 66 and 98 days and the masses in the Earth-size regime (see Table 1). Luckily, the two larger planets have the mean motions close to the 3:2 commensurability which result in observable deviations from a simple Keplerian description of the motion (Rasio et al. 1992; Malhotra et al. 1992; Peale 1993; Wolszczan 1994; Konacki et al. 1999). Konacki & Wolszczan (2003) applied the secular orbital theory of the PSR 1257+12 system motion from Konacki et al. (2000) to determine the masses and absolute inclinations of the orbits of the planets B and C. Recently, the same idea of incorporating the effects of mutual interactions between planets to remove the Doppler radial velocity (RV) signal degeneracy present in the  $N$ -Keplerian orbital model (i.e., the undeterminacy of the system inclination and the relative inclination of the orbits) has also been applied to study the strongly interacting, resonant system around Gliese 876 (Laughlin & Chambers 2001; Rivera & Lissauer 2001). However, the accuracy of the timing observations by far exceeds the precision of the RV measurements. In consequence, the accuracy of the PSR 1257+12 fit obtained by Konacki & Wolszczan (2003) and hence the corresponding initial condition is superior to any initial condition derived from the fits to RV observations of solar-type stars with planets. Thus, the system constitutes a particularly convenient and interesting subject for the studies of its dynamics.

There have been few and limited attempts to determine the long-term stability of the PSR 1257+12 system. Using the resonance overlap criterion and direct integrations, Rasio et al. (1992), Malhotra et al. (1992) and Malhotra (1993b) have found that the system disrupts in  $10^5$  yr timescale if the masses exceed about 2-3 masses of Jupiter. Also Malhotra et al. (1992) and Malhotra (1993a) have estimated that if the masses were about  $20 - 40 M_{\oplus}$  then the system would be locked in the exact 3:2 resonances which would lead to the TOA signal very different from what is actually observed. In this paper, we investigate the stability of the PSR 1257+12 system in the Gyr-scale. We also perform a dynamical comparison of the PSR 1257+12 system to the inner Solar System (ISS) as the dynamics of the ISS is mostly driven by interactions between

the telluric planets and is basically decoupled from the dynamics of the outer Solar System (Laskar 1994, 1997). Finally, we carry out a preliminary analysis of the stability of the orbits of massless particles (e.g. dust particles or Kuiper belt type objects) to determine the zones where such particles could survive and possibly be detected.

## 2. Numerical setup

The stability analysis performed in this paper has mostly numerical character and is understood in terms of the maximal Lyapunov Characteristic Number (LCN). Hence we treat the quasiperiodic orbital motions,  $LCN \simeq 0$ , as stable and the chaotic ones,  $LCN > 0$ , as unstable. In order to resolve the character of the orbits efficiently, we use the so-called fast indicator MEGNO (Mean Exponential Growth factor of Nearby Orbits, Cincotta & Simó 2000). It enables us to distinguish between regular and chaotic dynamics during integration of the studied system over only  $10^4$  orbital periods of the outermost planet. This feature is vital for examining large sets of initial conditions in the studies of exoplanetary dynamics (see e.g., Goździewski et al. 2001; Goździewski & Maciejewski 2003). The MEGNO is directly related to the LCN through the linear relation  $\langle Y \rangle = at + b$ . For quasiperiodic motions  $a \simeq 0$  and  $b \simeq 2$  while for chaotic solutions  $a \simeq (\lambda/2)$  and  $b \simeq 0$  where  $\lambda$  is the LCN of the orbit. However, there is no general relation between the magnitude of the LCN and the macroscopic changes of the orbital elements (e.g., Murison et al. 1994; Michtchenko & Ferraz-Mello 2001). Even if the LCN is large, the system can stay bounded for a very long time. More insight into the relation of the degree of the irregularity of motion and the macroscopic changes of the orbits one can obtain with the Modified Fourier Transform (MFT) developed by Laskar (1993). The MFT makes it possible to resolve the fundamental frequencies in a planetary system and to determine their diffusion rates (Robutel & Laskar 2001). In our tests, we use the MFT to verify the MEGNO integrations for massless particles (Section 4) and to identify the mean motion resonances (MMRs). During the computations of MEGNO, for every planet  $k = A, B, C$ , and also for massless particles ( $k = 0$ ) the complex functions  $f_k(t_i) = a_k \exp i\lambda_k(t_i)$ , have been computed at discrete times  $t_i$ , where  $t_{i+1} - t_i \simeq 10$  days, over the time  $2T$  between  $13,000 P_C$  and  $64,000 P_C$  (where  $P_C$  is the orbital period of the outermost planet C). Here,  $a_k$  denotes the semi-major axis of the relevant planet and  $\lambda_k$  is its mean longitude. For a quasi-periodic solution, the frequency corresponding to the largest amplitude,  $a_k^0$ , is one of the fundamental frequencies of motion, called the proper mean motion,  $n_k$  (Robutel & Laskar 2001). The 2-body MMRs can be identified through the condition  $q\mathbf{v}_i - p\mathbf{v}_j \simeq 0$ ,  $i \neq j = A, B, C, 0$ , where  $p, q > 0$  are prime integers. The MFT code gives us the rates  $\mathbf{v}_i/\mathbf{v}_j \simeq p/q$  and then  $p$  and  $q$  are found by the continued fraction algorithm. In this work we use the code which merges the MFT and MEGNO methods. It incorporates the MFT code which has been kindly provided by David Nesvorný<sup>4</sup>. For more details see Goździewski & Konacki (2003) and references therein.

In the numerical experiments, we use the initial condition given in Table 1. It represents one of the two fits obtained by Konacki & Wolszczan (2003) and has been transformed to the astrocentric elements. In

---

<sup>4</sup>[www.boulder.swri.edu/~davidn/fmft/](http://www.boulder.swri.edu/~davidn/fmft/)

the second orbital solution the inclinations are such that  $i_{B,C} \rightarrow 180^\circ - i_{B,C}$ . We assume that  $i_A$  obeys the same rule in that solution. It follows that both these solutions are dynamically equivalent and this reflects the fact that using the secular theory as the model of TOA measurements we are still not able to determine the absolute direction of the angular momentum vector. The TOA residuals exclude opposite directions of the outermost orbits (Konacki & Wolszczan 2003) hence the orbits are either prograde or retrograde.

### 3. Stability of the PSR 1257+12 planetary system

As the first numerical test, we have computed the MEGNO signature of the PSR 1257+12 system. This test has been repeated a few times with different, randomly selected initial variational vectors. The integrations were extended over about 500,000 yr corresponding to about  $2 \cdot 10^6 P_C$  which is significantly more than typically required  $\simeq 10^4$  of the characteristic periods (i.e.  $\simeq 10^4$  periods of the outermost planet). The results of a few of the runs are shown in Figs 1fe. Both the regular evolution of MEGNO,  $Y(t)$ , as well as the quick convergence of its mean value,  $\langle Y \rangle(t)$ , to 2, indicate a quasiperiodic motion. In some of the runs, after  $0.5 \cdot 10^6 P_C$  (see an example run marked with "x" in Fig. 1e) we have noticed a very slow divergence of the indicator from the theoretical value of 2. We can explain this by an accumulation of the numerical errors (Goździewski et al. 2001). Moreover, even if such a weak instability were to be understood in terms of the chaotic behavior, it would correspond to an extremely long Lyapunov time,  $T_L = 1/\lambda$ , comparable to  $10^9$  yr (estimated through the linear fit to the relation  $\langle Y \rangle = (\lambda/2)t + b$  over  $t \simeq 3.5 \cdot 10^6$  yr).

In Fig. 1, we also present the time-evolution of the orbital elements. Clearly, the motion of the planets B and C is tightly coupled. This is illustrated in panels a,b and c which show the variations of the osculating semi-major axes, eccentricities and inclinations. Fig. 1 d demonstrates the presence of a deep secular apsidal resonance (SAR), described by the critical argument  $\theta = \varpi_B - \varpi_C$  (where  $\varpi = \omega + \Omega$  is the longitude of periastron;  $\Omega$  and  $\omega$  are the longitude of ascending node and the argument of periastron of the planet, respectively), with a small semi-amplitude of the librations,  $\simeq 50^\circ$ , and apsides on average antialigned. In the discovery paper, Wolszczan & Frail (1992) have noticed the antialignment of the lines of apsides while Rasio et al. (1992) and Malhotra et al. (1992) have performed first theoretical explorations of the resonance. Surprisingly, the SAR has been recently found in many extrasolar systems discovered by the RV measurements. It is widely believed and justified that the SAR is crucial for maintaining the long term stability of multi-planetary exosystems involving Jupiter like planets (for an overview see, Ji et al. 2003). The fact that it is present both in planetary systems around main-sequence stars and around a neutron star may suggest that it is a common dynamical feature of exosystems.

Using the symplectic integrator WHM from the SWIFT package (Levison & Duncan 1994), we have also performed long term, 1 Gyr, integrations of the PSR 1257+12 system. The time step equal to 1 d resulted in the fractional error of the integrals of the angular momentum and the total energy at the level of  $\simeq 10^{-10}$ . During this interval no signs of instability are observed. We have not noticed any secular changes of the semi-major axes, eccentricities and inclinations. Their values stay within the limits shown in Fig. 1 and the SAR persists with an unchanged amplitude of librations (Fig. 2a) over 1 Gyr.

From the 1 Gyr integrations it follows that the orbital elements of the innermost planet A vary in a regular way (Fig. 1). However, we additionally detect a time evolution of the argument  $\theta_1 = \omega_A - \omega_B$  as a semi-regular sequence of rotations alternating with irregular "librations" about  $180^\circ$ . This effect is preserved over the entire period of 1 Gyr (see Fig. 2c,d). Such a behavior might indicate that the orbit crosses the separatrix of the secular resonance. This is illustrated in Figs 2c,d, which show the eccentricity of the planet A (multiplied by 10,000),  $e_A$ , plotted together with the argument  $\theta_1$ . Clearly, there is a correlation between the librations of  $\theta_1$  and small values of  $e_A$ . We also show  $e_C(\theta)$  and  $e_A(\theta_1)$  collected over the 1 Gyr integration (Fig. 2e,f). Obviously, the first case represents a trajectory in the resonant island of the SAR, whereas there is no clear sign of librations in the  $e_A(\theta_1)$  plot. This effect has only a geometrical nature and can be explained by estimating the secular frequencies of the system using the well known Lagrange-Laplace theory. If the MMRs are absent and the disturbing function is expanded up to the first order of the masses and to the second order of eccentricities and inclinations, the equations of secular motion are integrable. Their solution, relative to the eccentricities and longitudes of periastron, is given in terms of the so called eccentricity vectors,  $(h, k) = (e \sin \omega, e \cos \omega)$ , by (Murray & Dermott 2000)

$$\begin{aligned} h_j(t) &= \sum_i e_{j,i} \sin(g_i t + \beta_i) \\ k_j(t) &= \sum_i e_{j,i} \cos(g_i t + \beta_i), \end{aligned}$$

for every planet  $j = A, B, C$ . The constant amplitudes  $e_{j,i}$  and secular frequencies  $g_i$  are the eigenvectors and eigenvalues of a matrix with coefficients given explicitly in terms of the masses and constant semi-major axes of the planets. The scaling factors for the eigenvectors  $e_{i,j}$  and the phases  $\beta_i$  are determined by the initial condition. Geometrically, the time evolution of every eccentricity vector can be described as a superposition of the eigenmodes corresponding to  $g_i$  (Malhotra 1993b). The parameters obtained for the PSR 1257+12 system are given in Table 2. They are consistent with the results of Malhotra (1993a) and Rasio et al. (1992) who analyzed the PSR 1257+12 system involving the two larger companions. They found that the secular evolution of the eccentricity vectors of the two outer planets is almost entirely driven by the eigenstate corresponding to  $g_1$ . Since we have  $e_{B,1} \simeq -e_{C,1}$  and the other components of  $e_{j,i}$  are much smaller and almost equal, it follows that  $\omega_B \simeq \omega_C + 180^\circ$ , which corresponds to the SAR of the planets B and C. For the planet A, the eccentricity vector is a superposition of all the three eigenmodes with the leading second and third mode having comparable amplitudes. Curiously, we have  $g_1 - 7g_2 + 7g_3 \simeq 0.08 \text{ yr}^{-1}$ . It appears that with this relation we can explain the semi-librations of  $\theta_1$ . The minima of  $e_A$  occur when the modes corresponding to the frequencies  $g_2$  and  $g_3$  are in antiphase. Because the amplitudes  $e_{A,2}$  and  $e_{A,3}$  have the same sign and similar magnitudes while  $e_{A,1}$  has a much smaller magnitude, the following condition has to be satisfied to grant a minimum of  $e_A$

$$(g_2 t + \beta_2) - (g_3 t + \beta_3) \simeq (2m + 1)180^\circ, \quad m \geq 0$$

Since  $\beta_2 - \beta_3 \simeq -180^\circ$  (see Table 2), we have  $(g_2 - g_3)t = m360^\circ, m \geq 0$  and the period of antialignment is  $P_{23} = 360^\circ/(g_2 - g_3) \simeq 43,000 \text{ yr}$ . From the relation between the  $g_i$ , this period is almost commensurate with  $P_1$  (where  $P_1 = 360^\circ/g_1$ ). Near the moment of antialignment, the eccentricity of the planet A,  $e_A$ , is driven mostly by the  $g_1$ -mode that is in antiphase with the eccentricity vector for  $e_B$ . This leads to the quasi-librations seen in Fig. 2 as they repeat with the same period as the variations of  $e_A, P_{23}$ .

So far we have been falsely assuming that the MMRs are absent. Therefore to estimate the influence of the near 3:2 MMR on the secular solution, we integrated the system for 10 Myr, sampling the orbital elements every 100 yr. Next, MFT was applied to analyze the complex signals  $e_p \exp(i\omega_p)$ . In this way, we can obtain an estimate of the precessional frequencies  $g_p$ . These frequencies, corresponding to the dominant amplitudes and measured in arcsec/yr, are  $\simeq 197.742$ ,  $\simeq 43.881$  and  $\simeq 13.157$ . The first one is substantially different from its analytical counterpart what will lead to a fast discrepancy between the analytical and numerical solutions. This discrepancy proves, that the classical secular theory has to be modified in order to account for the near 3:2 MMR effects. Such a theory has been already developed by Malhotra et al. (1989) for the satellites of Uranus. It can be applied to the PSR 1257+12 system too, however this is out of the scope of this paper.

### 3.1. Comparison to the inner Solar System

The results of the 1 Gyr integration enable us to analyze the time-evolution of the so-called Angular Momentum Deficit (AMD, Laskar 1997):

$$C = \sum_{p=A,B,C} \frac{m_p m_*}{m_p + m_*} \sqrt{\mu_p a_p} (1 - \sqrt{1 - e_p^2} \cos i_p),$$

where  $\mu_p = G(m_p + m_*)$ ,  $G$  is the gravitational constant,  $a_p, e_p, i_p$  is the semi-major axis, eccentricity and inclination of a planet relative to the invariant plane and  $m_*$  is the mass of the central body. The AMD indicates the deviation of planetary orbits from a stable circular and coplanar motion for which  $C = 0$ . This quantity is preserved by the averaged equations of motion (Laskar 1997) and its stability provides the stability of the secular system in the absence of short-period resonances. The AMD can be understood as the amplitude of the irregularity present in the averaged system. Large values of AMD lead to a chaotic motion and for a certain critical value to a crossing of the orbits and the disruption of a planetary system (Laskar 1997, 2000; Michtchenko & Ferraz-Mello 2001).

The PSR 1257+12 system is close to the 3:2 commensurability. Its critical argument circulates but it does not mean that the time-averaged effects of the near-resonance vanish (Malhotra et al. 1989; Malhotra 1993a). Hence, the applicability of the AMD signature in the studies of the stability in the real, unaveraged system can be problematic. Nevertheless, we have decided to calculate the AMD and to examine its behavior. Its time evolution is shown in Fig. 5. The AMD stays well bounded and very regular. There is very little exchange of the AMD between the innermost planet A and the pair of the bigger companions B and C. It suggests that the motion of the planet A is decoupled from the dynamics of the planets B and C in the long-term scale. This situation is qualitatively different from the inner Solar system (ISS). The AMD of the ISS is not strictly preserved due to the perturbations of Jupiter and Saturn, nevertheless it can be considered roughly constant (Laskar 1997; Ito & Tanikawa 2002). Ito & Tanikawa (2002) have recently published the results of 5 Gyr integrations of the ISS which reveal a rapid AMD variations of Mercury, much larger than the changes of AMD of the Venus-Earth pair. The variations of the AMD of Venus, Earth and Mars are also irregular and substantial. In fact, the ISS is chaotic having the Lyapunov time about 5 Myr (Laskar 1994). Laskar

(1994) has also found that this chaos is physically significant as it can lead to the ejection of Mercury from the inner ISS during a few Gyr. However, the source of chaos in the ISS is still not well understood (Lecar et al. 2001). In this sense, the character of the motion of the PSR 1257+12 system is quite different. The evolution of its AMD is very regular in spite of smaller distances, larger masses and thus stronger mutual interactions between the planets. Unlike Mercury’s, the AMD of the planet A is negligible when compared to the AMD of the B-C pair as it contributes only about 1/1000 of the total value. On the other hand, the orbital coupling of the pairs B-C and Venus-Earth (Ito & Tanikawa 2002) is a similar feature of the inner Solar and PSR 1257+12 systems although it has a different nature. The primary factor for the stability of the B-C pair could be the antialigned SAR which “keeps” the planets away on their orbits and provides the well behaved AMD. The chaotic orbital evolution of the ISS may significantly depend on the weak coupling with the outer planets. An equivalent effect is obviously absent in the PSR 1257+12 system.

### 3.2. Dynamical environment of the PSR 1257+12 planetary system

In the next experiments we look at the initial condition in a global manner in order to find out whether the current state of the system is robust to adjustments of the initial condition (IC). However, thanks to a very precise determination of the initial condition such changes, if considered consistent with the TOA measurements, are very limited. For example, the formal  $1\sigma$  error of the semi-major axes inferred from the parameter  $x^0$  (Konacki & Wolszczan 2003) is at the level of  $10^{-6}$  AU! Nevertheless, the localization of the IC in the phase space (for instance its proximity to unstable regions) is very important to determine or confirm its character. The examination of one isolated IC does not provide a definitive answer to the question of stability.

We computed one-dimensional scans of MEGNO,  $\langle Y \rangle$ , by changing the semi-major axes of one planet and keeping the other orbital parameters fixed at the values given in Table 1. The results of this experiment are illustrated in Fig. 3. The MEGNO scans reveal a number of spikes. Most of them can be identified as 2-body MMRs between the planets. Currently, the IC is well separated from the low-order resonances. Some unstable high-order MMRs appear close to the nominal initial condition. The most relevant one seems to be the 31:21 MMR between the planets B and C (see the bottom panel in Fig. 3). Yet such resonances are extremely narrow and it is unlikely that they can affect the regular motion of the system. Figure 4 shows the effect of varying the assumed mass of the neutron star on the determination of the semi-major axis of the outermost planet and the localization of the resonances. Obviously, the sequence of MMRs does not change. A different mass of the pulsar can lead to a substantial shift of the initial semi-major axis (in our case,  $a_C$ ) and the weak unstable resonances, like the 31:21 MMR, may end up much closer to the nominal positions of the planets (for smaller than canonical mass of the parent star).

The one-dimensional scans help us interpret the results of the 2-dimensional MEGNO analysis which is shown in Fig. 5. In all cases the nominal IC, marked by the crossed lines, is localized in wide stable regions. This is seen in the  $(e_B, e_C)$ -plane. In the  $(a_B, a_C)$ -plane (the middle panel), the thin strips of the MMRs can be easily identified. This also concerns the  $(a_B, e_B)$ -map which additionally reveals the width of the most

relevant MMRs like the 3:2, 13:9 and 10:7. These stability maps confirm that the nominal quasiperiodic PSR 1257+12 system is located far from strong instabilities of the motion in an extended zone of stable dynamics.

During the MEGNO integrations we have also computed the maximum value of the critical argument  $\theta = \varpi_B - \varpi_C$  with respect to the libration center of  $180^\circ$ . It enables us to estimate the semi-amplitude of librations and the extent of the SAR in the space of the scanned orbital parameters. The result of such an experiment conducted in the  $(e_B, e_C)$  plane are shown in Fig. 6. It uncovers an extended zone of the SAR with the smallest semi-amplitude of  $\theta$  in the vicinity of the nominal initial condition of the PSR 1257+12 system. The near 3:2 MMR is also clearly present in this map.

After Konacki & Wolszczan (2003), we are using the average inclination of the orbits of the planets B and C as the orbital inclination of the planet A. However, we have tried to verify whether the dynamics can provide any limits on the inclination and mass of the innermost planet A. In the experiment, we have changed the inclination of the planet in the range  $[10^\circ, 90^\circ]$  and the position of the nodal line over  $360^\circ$  — thus varying both the mass as well as the relative inclination of the planet A to both orbital planes of the planets B and C. No instability has been detected and it seems that the dynamics cannot be used to constrain the inclination and mass of the innermost planet A. It reflects the fact the the planet A is dynamically decoupled for the pair B-C as we have found it analyzing the AMD.

#### 4. Dynamics of massless particles

While investigating the dynamics of extrasolar planetary systems one can ask whether the minor bodies can survive in the gravitational environment of the giant primary bodies. These can be small telluric planets in the exosystems with Jupiter-like planets. We can ask the same question about asteroids, cometary bodies or dust particles in the PSR 1257+12 system. Because the motion of the planets appears to be strictly stable, we can consider a simplified, restricted model. In this model one assumes that a probe mass moves in a gravitational tug of the primaries but does not influence their motion. In the simplest case such a model is well known as the restricted, planar circular three body problem (Murray & Dermott 2000). This simplification helps us to explore the phase space of the planetary system with reasonable computational effort. In this model, the MEGNO indicator and the MFT are evaluated only for the probe mass. In the numerical experiments, we investigate the orbital stability of massless particles in a few regions of the orbital space: between the planets A and B (region I), B and C (region II) and beyond the planet C (region III).

In the first series of numerical tests, we vary the initial semi-major axis of the probe mass,  $a_0$ , and its eccentricity,  $e_0$ , while the initial inclination is constant,  $i_0 = 50^\circ$ . Thus the tested orbits are slightly inclined to both orbital planes of the planets B ( $i_B = 53^\circ$ ) and C ( $i_C = 47^\circ$ ). The angular variables of the massless particles are set to  $\Omega_0 = \varpi_0 = M_0 = 0^\circ$ . This way we essentially follow the remarkable work of Robutel & Laskar (2001) who investigated the short-term dynamics of massless particles in the Solar System using the MFT. These authors argue that the global picture of the motion in the restricted problem does not

qualitatively depend on the initial phases of the test particle. The initial plane  $(a_0, e_0)$  is representative for the dynamics because it crosses all resonances. By changing the initial orbital phases of the massless particles, the width of the resonances may vary but their influence on the motion can still be detected.

In order to check the MEGNO signatures (e.g., to verify whether the integration time is not too short), during the integrations, we compute the diffusion rate,  $\sigma_0 = 1 - n^{(2)}/n^{(1)}$ , where  $n^{(1)}$  and  $n^{(2)}$  are the mean motion frequencies<sup>5</sup> obtained over the intervals  $[0, T]$  and  $[T, 2T]$ , respectively, where  $T$  (which we will call the base period from hereafter) has been set accordingly to the investigated range of the semi-major axes. The close encounters with the planets are controlled. We assume that if the distance between the probe mass and a planet is less than the Hill radius,  $r_H = [m_p/(3m_*)]^{(1/3)}a_p$ , then the particle has collided with the planet or its motion become strongly chaotic.

Within this numerical setup, in the region II we have not detected any stable motions. The region I turns out to be a much more interesting one. The results are shown in the MEGNO and  $\sigma$  maps in Fig. 7 (left panels for the region I, middle and right panels for the region III). The integrations have been carried out for the total time,  $2T$ , of about 32,000  $P_C$ . In both maps we can clearly recognize the planetary-crossing lines marked by large values of both indicators which correspond to strongly chaotic motions. These lines (white lines in Fig. 7) are the solutions to the equations  $a_p(1 + e_p) = a_0(1 - e_0)$  for  $a_0 > a_p$  and  $a_p(1 - e_p) = a_0(1 + e_0)$  for  $a_0 < a_p$  where  $a_p, e_p, a_0, e_0$  denote the initial semi-major axis and the eccentricity of a planet and a test particle, respectively.

In this area and above the collision lines, the particles are scattered mostly by close-encounters and collisions with the planets A and B. Remarkably, a stable area exist under the crossing-lines with the planets A and B. It is divided by a number of MMRs with the planets. In order to verify this result, we have integrated the motion of 200 particles spread over  $[0.19, 0.35]$  AU with the same resolution in the semi-major axis,  $a_0$ , as in the 2D MEGNO test. These integrations were continued up to 15 Myr (here, we used the RMVS3 integrator from the SWIFT package). A resulting one dimensional scan of MEGNO over  $a_0$  is shown in Fig. 8. In the regions classified with MEGNO as regular, the massless particles have mostly survived during the integration time while in the chaotic or close to chaotic areas, they have been quickly removed or collided with the planets (in this test the same criterion of 1 Hill radii for a collision event is used and in such a case we set  $\log \sigma_0 = 1$ ). Some discrepancies are most likely related to the different integrators used in the experiment; the Bulirsh-Stoer integrator follows the orbits of massless particles much more accurately than the symplectic integrator does. This experiment enables us also to independently estimate the proper MEGNO integration time and to "calibrate" the scale of the diffusion rate,  $\sigma_0$ . Comparing the MEGNO and  $\sigma_0$ -maps, we conclude that for  $\log \sigma$  less than about  $(-7)$ – $(-8)$  the motion can be considered as regular (also compare the maps in the left column of Fig. 7). Let us note that both indicators are in an excellent accord and the diffusion rate calculated by the MFT algorithm seems to be even more sensitive to

---

<sup>5</sup>Note, in order to derive rigorous estimates of the *proper* mean motion frequencies one has to employ angle-action like coordinates, e.g. the Poincaré variables (Laskar & Robutel 1995) or the Jacobi coordinates. In this sense, we cannot refer in this test to the proper frequencies because our integrations have been carried out in astrocentric coordinates and the osculating elements analyzed by MFT are inferred from these non-canonical coordinates.

an unstable motion than the MEGNO is.

Using a similar numerical setup, we have investigated the region III. However, due to an extended range of the semi-major axes, we have divided it into two parts: the region IIIa between 0.5 AU and 0.97 AU and the region IIIb between 0.9 AU and 3.9 AU (a distance comparable to the radius of the Asteroid Belt in the Solar System). The maps of MEGNO and the diffusion rate,  $\log \sigma$ , in the  $(a_0, e_0)$ -plane for the region IIIa (obtained after the time  $2T \simeq 32,000$  P<sub>C</sub>), are shown in the middle column of Fig. 7 while the maps for the region IIIb ( $2T \simeq 64,000$  P<sub>C</sub>) are shown in the right column. For the region IIIa, in both maps, we can clearly recognize the collision line with the outermost planet while the crossing line with planet B is in the zone of strong chaos. A net of MMRs appears as narrow vertical strips. This test shows that for a moderately low initial eccentricity,  $e_0$ , the stable zone is extended and begins just beyond the orbit of the planet C. Obviously, with a growing  $e_0$  the border of the stable zone shifts towards a larger  $a_0$  (at the distances of about 1 AU the zone of stability reaches  $e_0 \simeq 0.5$ ). For the region IIIb ( $a_0 \in [0.9, 3.9]$  AU), the results are shown in the right column of Fig. 7. For efficiency reasons, in this test the step in  $e_0$  is 0.1 (the resolution in  $a_0$  has been left relatively high, at 0.005 AU). The collision lines are clearly present. Otherwise, this zone is mostly regular even for very large  $e_0 > 0.5$ . Similarly to the region IIIa, the scans reveal some extremely narrow unstable MMRs, most of them with the two outer planets.

Finally, we examined the stability of orbits inclined to the mean orbital plane of the system. In this experiment we tested the motion of particles in the region III. The results for the region IIIa are shown in Fig. 9 (a number of additional scans, not shown here, allows us to extrapolate the results obtained for this region to the region IIIb). In the first two experiments, we scanned the  $(a_0, e_0)$  space for the initial  $i_0$  set to 75° and 87°, respectively. These inclinations, taken relative to the mean orbital plane of the PSR 1257+12 system, are comparable to inclinations of Kuiper belt objects in the Solar System. Again, the collision lines and the net of MMRs clearly appear in both the MEGNO and  $\sigma_0$  scans which are shown in the left and the middle panels of Fig. 9. The zone of strong chaos covers the crossing zones with the planets B and C while the collision line with the planet A is much more narrow and separated by a quasi-regular area in which  $\sigma_0 \simeq 10^{-6}$ . Such an effect has been already observed by Robutel & Laskar (2001) — for higher inclination the close encounters with the planets are less frequent than for moderately small inclinations which explains the smaller extent of the strong chaos. Moreover, after sufficiently long time the massless bodies will be removed from above the collision lines, excluding cases when the probes are trapped within stable MMRs. In the next test illustrated in the right panel of Fig. 9,  $e_0$  has been fixed to 0 and the initial inclination  $i_0$  has been varied in the wide range [10°, 90°]. This experiments allows us to generalize the results of the previous scans. The stability of inclined particles is basically independent on the initial inclination, at least for moderately small eccentricities.

One should be aware that the results of the above analysis should be treated as preliminary ones. Our study is restricted both to the short-term dynamics and a small part of the possible volume of the parameter space. However, the timescale of the integrations is long enough to detect the most unstable regions in the phase space and to point out the regions where the particles can be long-term stable. Also in some chaotic regions the particles can still persist over a very long time but this can be verified only by direct integrations.

## 5. Conclusions

In this work we carry out numerical studies of the stability of the PSR 1257+12 system using the initial condition determined by Konacki & Wolszczan (2003). The long term integrations utilizing the symplectic integrator, extended over 1 Gyr, do not reveal any secular changes in the semi-major axes, eccentricities and inclinations of the planets. Using the notion of the Angular Momentum Deficit (AMD), we do not find any substantial exchange of the angular momentum between the innermost planet and the pair of the outer, bigger planets B and C. The AMD of the planet A is negligible when compared to the AMD of the B-C pair. This is very different from the case of the inner Solar System in which the variations of the AMD of Mercury are the most significant ones. The PSR 1257+12 system has the MEGNO signature characteristic for a strictly regular, quasi-periodic configuration. The two outer planets are close to the 3:2 mean motion resonance and are orbitally tightly coupled. The primary key for maintaining their stability is most likely the secular apsidal resonance with the semi-major axes on average antialigned. The semi-amplitude of the critical argument of this resonance is about  $50^\circ$  and it persists in a wide range of the orbital initial parameters. The SAR in the PSR 1257+12 system is yet another case of such a resonance in the extrasolar planetary systems (Ji et al. 2003). The current statistics may not be sufficient but the frequency of occurrences of the SAR is striking. It may reflect a more general rule which the extrasolar planetary systems follow.

The neighborhood of the nominal initial condition is verified by calculating the MEGNO signature in a few representative planes of initial semi-major axes and eccentricities of the planets. These stability maps reveal that the nominal initial condition is located in an extended stable zone, relatively far from any strong instabilities of the motion. These factors allows us to state that the PSR 1257+12 system is orbitally stable over Gyr time scale. In our experiments, there are no signs of a potential instability except for a very slow divergence of the MEGNO in few of the test. This divergence of MEGNO corresponds to the Lyapunov time of about  $\simeq 1$  Gyr. We believe that most likely it has only a numerical character but it might deserve a closer look.

We are aware that an alternative analytical study of the PSR 1257+12 dynamics is possible (also thanks to the accurate determination of the initial condition). Such an approach has been derived in Malhotra et al. (1989) and Malhotra (1993a). Our numerical investigations can certainly be treated as a complement to future analytical studies of the system.

Finally, using the MEGNO and the MFT, we investigate the dynamics of massless particles in the PSR 1257+12 system in the framework of the restricted model. In the numerical experiments, we find a stable zone between the planets A and B extending for initially small eccentricities from 0.19 AU to 0.25 AU from the pulsar. There are no stable areas between the planets B and C. Beyond the orbit of the planet C, the stable zone begins already outside of its orbit. We find that the massless particles can move on stable orbits under the condition that their initial eccentricities and semi-major axes are located under the collision lines with the planets. The dynamics of massless particles is basically independent on the their initial inclinations. Beyond 1 AU, the motion appears to be stable except for the areas of narrow MMRs with the planets B and C. It is an encouraging result supporting the search for possible small bodies contained in a dust or Kuiper belt type disk around the PSR 1257+12.

## 6. Acknowledgments

We thank Philippe Robutel for discussions and helpful remarks. K. G. is supported by the Polish Committee for Scientific Research, Grant No. 2P03D 001 22. M. K. is a Michelson Postdoctoral Fellow.

## REFERENCES

Cincotta, P. M. & Simó, C. 2000, A&AS, 147, 205

Goździewski, K. & Konacki, M. 2003, ApJ, astro-ph/0307501

Goździewski, K. & Maciejewski, A. J. 2003, ApJ, 521

Goździewski, K., Bois, E., Maciejewski, A., & Kiseleva-Eggleton, L. 2001, A&A, 378, 569

Hairer, E. & Wanner, G. 1995, <http://www.unige.ch/math/folks/hairer/>

Ito, T. & Tanikawa, K. 2002, MNRAS, 336, 483

Ji, J., Liu, L., Kinoshita, H., Zhou, J., Nakai, H., & Li, G. 2003, ApJ, 591, L57

Konacki, M., Maciejewski, A. J., & Wolszczan, A. 1999, ApJ, 513, 471

—. 2000, ApJ, 544, 921

Konacki, M. & Wolszczan, A. 2003, ApJ, 591, L147

Laskar, J. 1993, Celest. Mech. & Dyn. Astr., 56, 191

—. 1994, A&A, 287, L9

—. 1997, A&A, 317, L75

—. 2000, Physical Review Letters, 84, 3240

Laskar, J. & Robutel, P. 1995, Celest. Mech. & Dyn. Astr., 62, 193

Laughlin, G. & Chambers, J. E. 2001, ApJ, 551, L109

Lecar, M., Franklin, F. A., Holman, M. J., & Murray, N. J. 2001, ARA&A, 39, 581

Levison, H. F. & Duncan, M. J. 1994, Icarus, 108, 18

Malhotra, R. 1993a, in ASP Conf. Ser. 36: Planets Around Pulsars, 89–106

Malhotra, R. 1993b, ApJ, 407, 266

Malhotra, R., Black, D., Eck, A., & Jackson, A. 1992, Nature, 356, 583

Malhotra, R., Fox, K., Murray, C. D., & Nicholson, P. D. 1989, A&A, 221, 348

Michtchenko, T. & Ferraz-Mello, S. 2001, ApJ, 122, 474

Murison, M. A., Lecar, M., & Franklin, F. A. 1994, AJ, 108, 2323

Murray, C. D. & Dermott, S. F. 2000, Solar System Dynamics (Cambridge Univ. Press)

Peale, S. J. 1993, AJ, 105, 1562

Rasio, F. A., Nicholson, P. D., Shapiro, S. L., & Teukolsky, S. A. 1992, Nature, 355, 325

Rivera, E. J. & Lissauer, J. J. 2001, ApJ, 402, 558

Robutel, P. & Laskar, J. 2001, Icarus, 152, 4

Wolszczan, A. 1994, Science, 264, 538

Wolszczan, A. & Frail, D. A. 1992, Nature, 355, 145

Fig. 1.— The orbital evolution of the nominal PSR 1257+12 system and its MEGNO signature. Panel (a) is for the semi-major axes. Panel (b) is for the orbital inclinations. Panel (c) is for the eccentricities. Panel (d) illustrates the secular apsidal resonance between the planets B and C. Panels (f) and (e) are for the time-evolution of MEGNO and its mean value,  $\langle Y \rangle(t)$  (a few representative evolutions for different choices of the initial tangent vector are shown and an example of a slowly divergent solution is marked with "x").

Fig. 2.— The dynamics of the PSR 1257+12 system in the 1 Gyr integration. Panel (a) is for the critical argument of the secular apsidal resonance during the first 275 Myr. Panel (b) is for the AMD. Panels (c) and (d) are for the argument  $\theta_1 = \varpi_A - \varpi_B$ . Panel (c) is for the first 2 Myr while panel (d) is for the end of the 1 Gyr period. The orbital evolution illustrated in panel (c) is obtained with a very precise integrator ODEX (Hairer & Wanner 1995) and the relative and absolute accuracy set to  $10^{-14}$  and  $5 \cdot 10^{-16}$ , respectively. The solid line in these plots denotes the eccentricity of the innermost planet multiplied by  $10^4$ . Panel (e) shows the SAR between the planets B and C in the space of  $(\varpi_A - \varpi_B, e_C)$ . The same plot for  $\theta_1$  and  $e_A$  is shown in panel (f).

Fig. 3.— The dynamical environment of the PSR 1257+12 planets in the space of the semi-major axes. The plots are for the one-dimensional MEGNO scans along the semi-major axis of the planet A, B and C. All the other initial elements are fixed at their nominal values (see Table 1). The resolution of the scans is 2400 data points in every plot. Labels mark the positions of the MMRs between the planets: the upper plot for the A-B pair (bold labels) and A-C (regular labels), the second, the third, and the fourth panel from the top for the B-C pair. The bottom plot is a magnification of the scan for the planet C. Big dots mark the nominal positions of the planets.

Fig. 4.— The MEGNO scan over  $a_C$  for different masses of the host star. The upper scan is for  $m_\star = 0.95M_{\text{psr}}$  and the lower for  $m_\star = 1.05M_{\text{psr}}$  where  $M_{\text{psr}}$  is the canonical mass of the pulsar,  $1.4 M_\odot$ .

Fig. 5.— The MEGNO stability maps for the configuration given in Table 1. The left panel is for the  $(e_B, e_C)$  plane. The middle panel is for the  $(a_B, a_C)$  plane. The right panel is for the  $(a_B, e_B)$  plane. The position of the nominal system is marked by the two intersecting lines.

Fig. 6.— The semi-amplitude  $\theta^{\max}$  of the SAR in the  $(a_B, e_B)$ -plane. The position of the nominal system is marked by two intersecting lines.

Fig. 7.— The MEGNO scan over the semi-major axis  $a_0$  of the massless particles moving between the planet A and B (thick line) and their survival times over 15 Myr integrations (represented by thin vertical lines).

Fig. 8.— The stability maps for the massless particles moving in different regions of the PSR 1257+12 system. The left column is for the region II (between the planets A and B), the middle panel is for the region IIIa (beyond the planet C, up to 1 AU) and the right panel is for the region IIIb (up to 3.9 AU). The upper maps are for MEGNO, the bottom maps are for the diffusion rate  $\log \sigma_0$ . The resolution of the scans is  $0.0008\text{AU} \times 0.005$ ,  $0.0025\text{AU} \times 0.005$  and  $0.005\text{AU} \times 0.1$ , respectively. Collision lines with the planets are marked with white curves.

Fig. 9.— The stability maps for the massless particles moving in the region IIIa of the PSR 1257+12 system for different initial inclinations. The left column is for the initial inclination  $i_0 = 75^\circ$ , the middle column is for  $i_0 = 87^\circ$ . The right panels are for  $e_0 = 0$  and  $i_0 \in [10^\circ, 90^\circ]$ . The upper maps are for MEGNO, the bottom maps are for the diffusion rate  $\log \sigma_0$ . The resolution of the scans is  $0.0023\text{AU} \times 0.04$ ,  $0.0019\text{AU} \times 0.01$ , and  $0.0019\text{AU} \times 2^\circ$ , respectively.

Table 1. Astrocentric osculating orbital elements of the planets in PSR 1257+12 planetary system at the epoch MJD=49766.50.<sup>a</sup>

Planet	Mass [M <sub>⊕</sub> ]	<i>a</i> [AU]	<i>e</i>	<i>i</i> [deg]	Ω [deg]	ω [deg]	<i>M</i> [deg]
A	0.019	0.18850	0.0000	50.00	0.00	0.0	14.25
B	4.250	0.35952	0.0186	53.00	0.00	250.4	5.41
C	3.873	0.46604	0.0252	47.00	3.26	108.3	3.66

<sup>a</sup> The semi-major axis, *a*, the eccentricity, *e*, the inclination, *i*, the longitude of ascending node, Ω, the argument of periastron, ω, and the mean anomaly, *M*, of the planets in PSR 1257+12 planetary system at the epoch MJD=49766.50 are derived from the best-fit orbital parameters by Konacki & Wolszczan (2003). The mass of the central star is equal to 1.4 M<sub>⊙</sub>.

Table 2. Parameters for the (*h*,*k*) secular solution obtained by means of the Lagrange-Laplace theory. Amplitudes *e<sub>p,i</sub>* are multiplied by 10<sup>3</sup>.

Mode [i]	<i>g</i> [arcsec/yr]	β [deg]	<i>e<sub>A,i</sub></i>	<i>e<sub>B,i</sub></i>	<i>e<sub>C,i</sub></i>	Period [yr]
1	209.991	272.28	-2.075	21.148	-20.311	6171.7
2	44.713	140.17	-8.146	0.010	0.013	28984.7
3	14.061	333.01	-6.928	-7.937	-7.960	92169.0

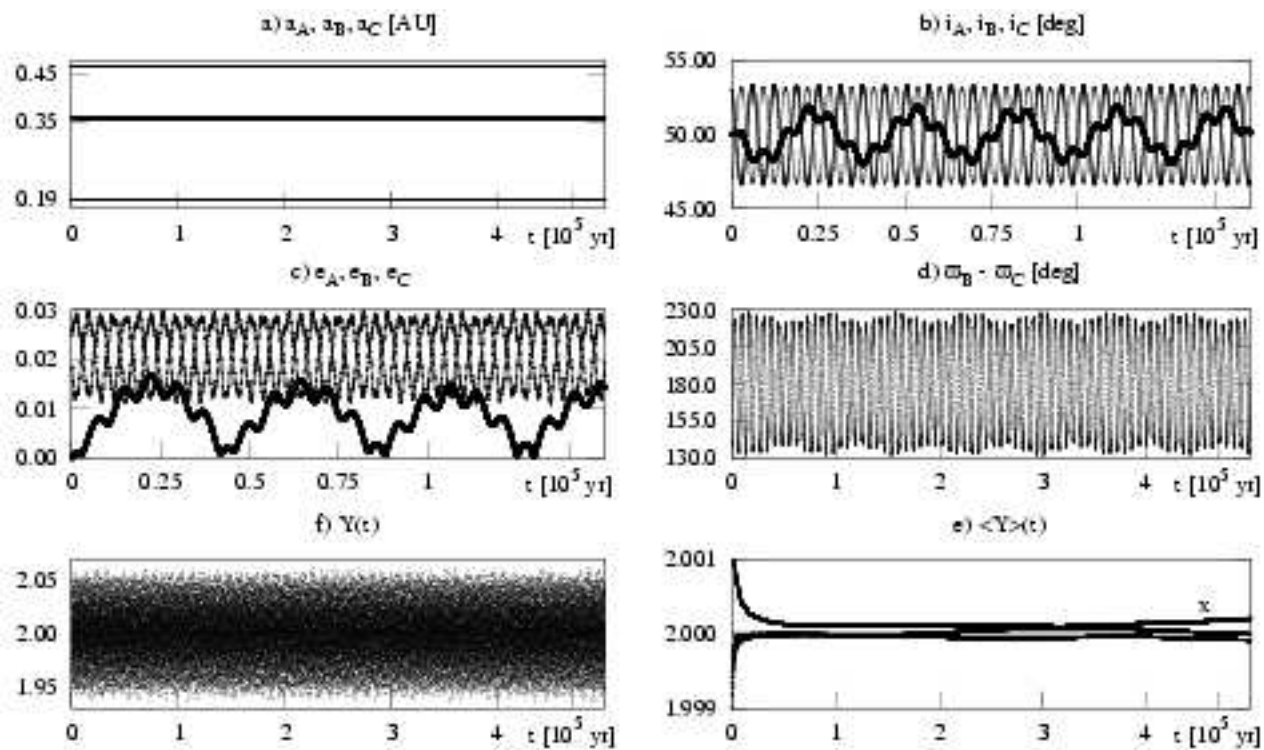


Fig. 1.—

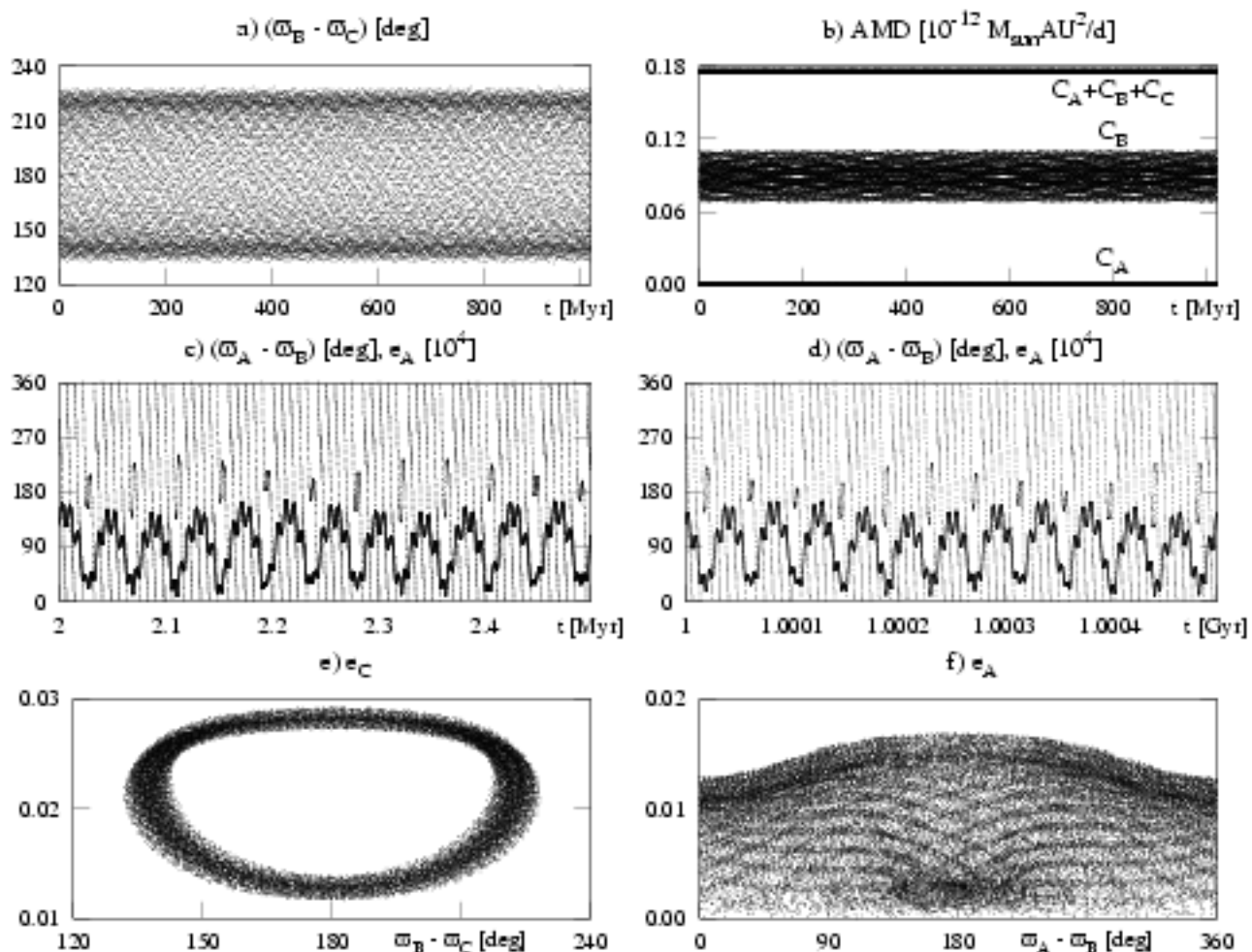


Fig. 2.—

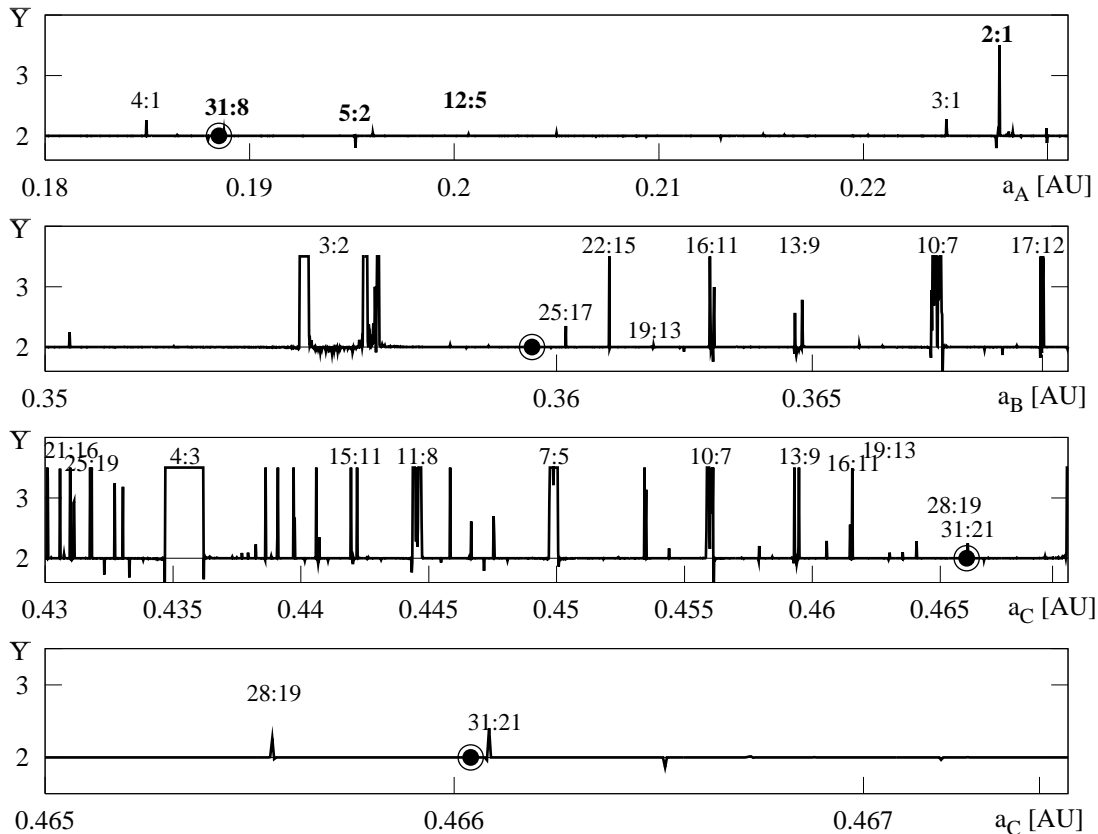


Fig. 3.—

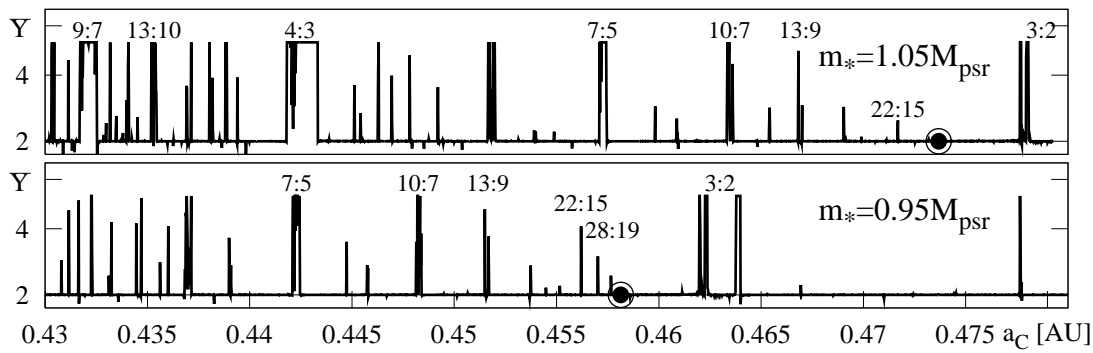


Fig. 4.—

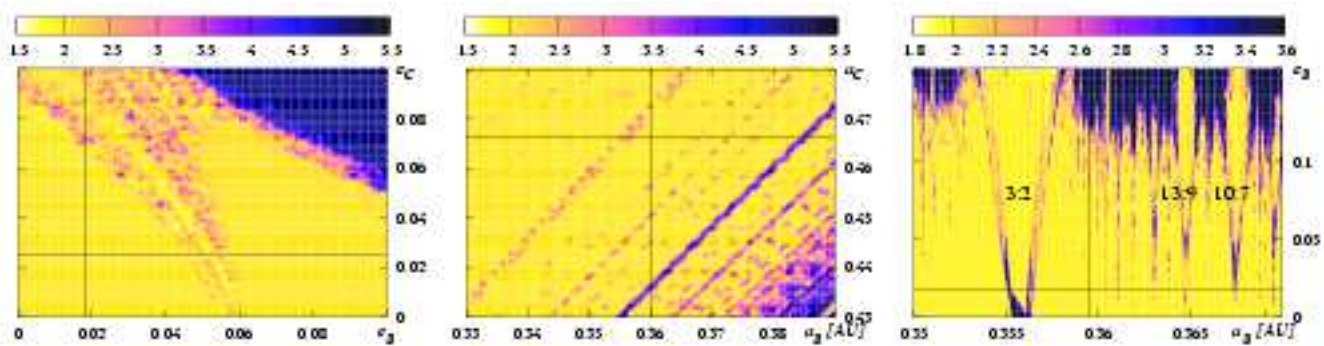


Fig. 5.—

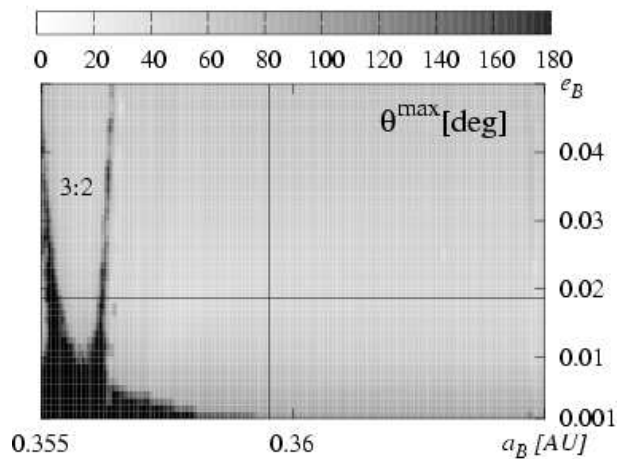


Fig. 6.—

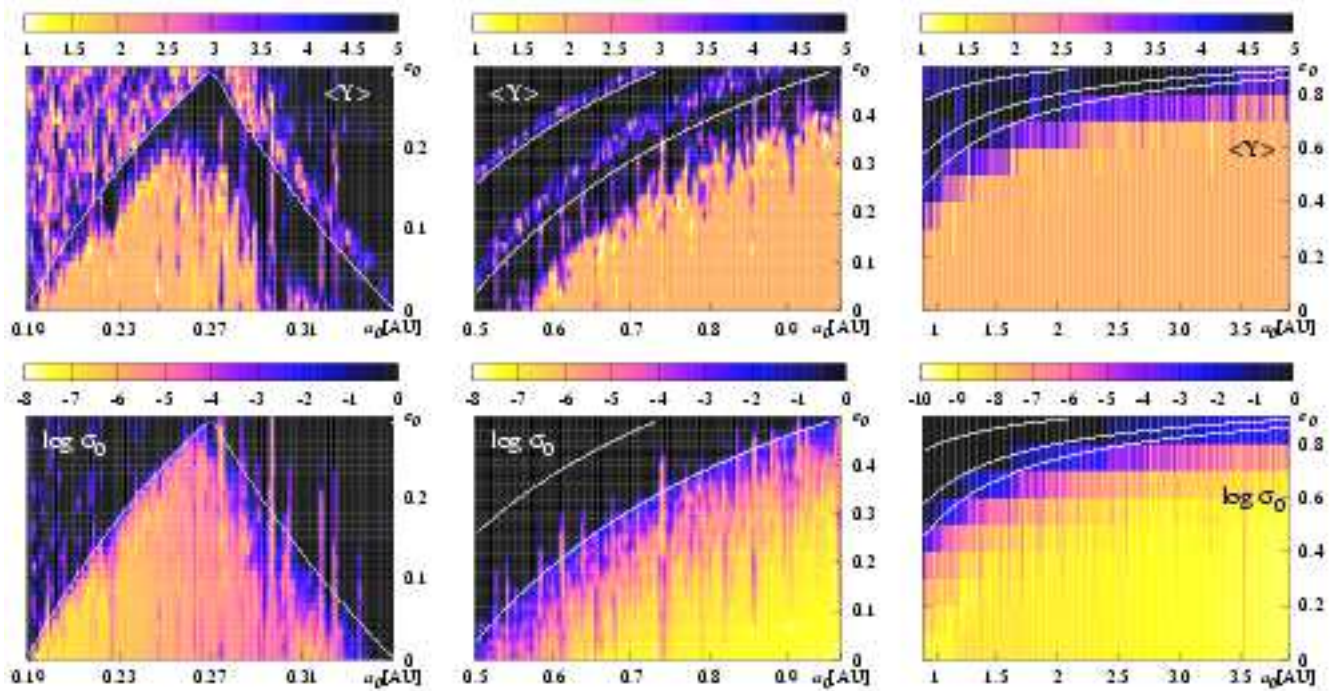


Fig. 7.—

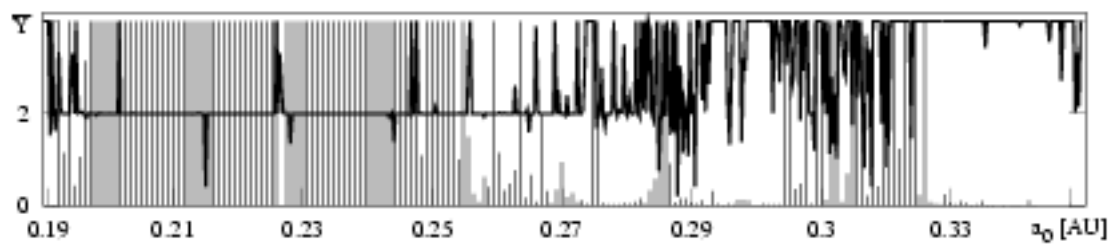


Fig. 8.—

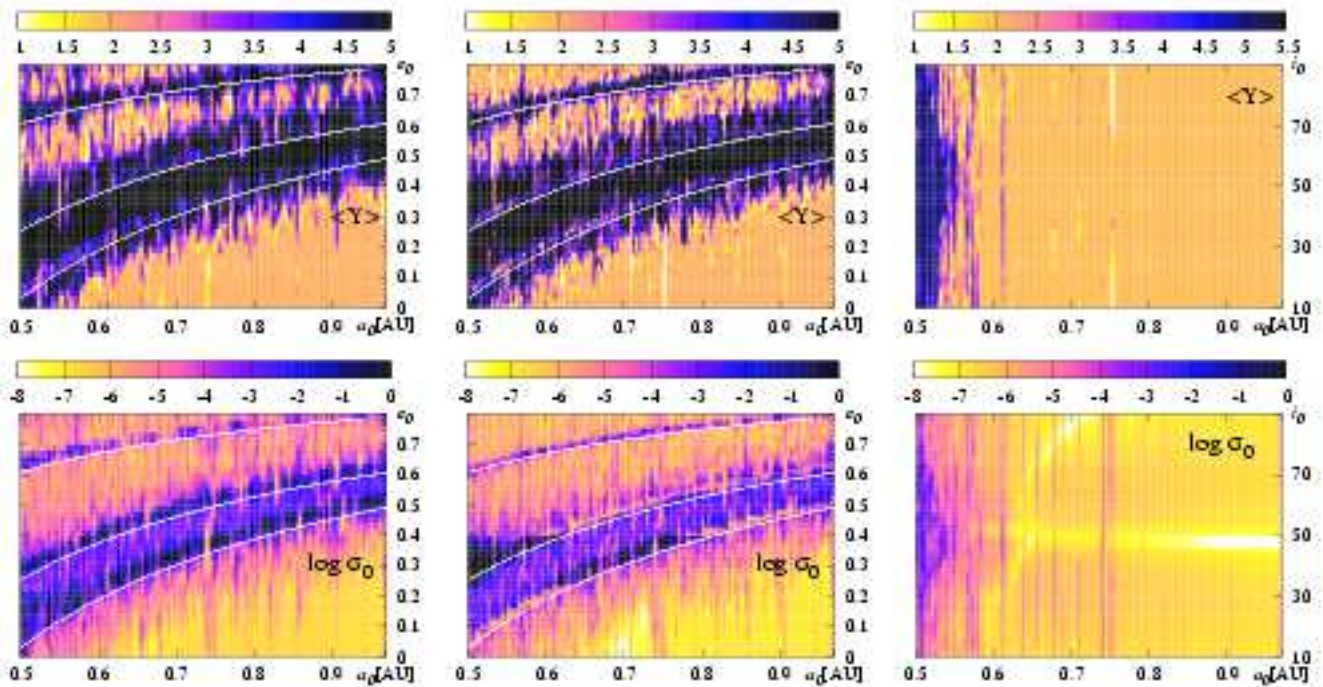


Fig. 9.—